Novel function of keratins 5 and 14 in proliferation and differentiation of stratified epithelial cells

Hunain Alam, Lalit Sehgal, Samrat T. Kundu, Sorab N. Dalal, and Milind M. Vaidya
Advanced Centre for Treatment, Research & Education in Cancer (ACTREC), Tata Memorial Centre, Kharghar, Navi Mumbai 410210, India

ABSTRACT **Keratins are cytoplasmic intermediate filament proteins preferentially expressed by epithelial tissues in a site-specific and differentiation-dependent manner. The complex network of keratin filaments in stratified epithelia is tightly regulated during squamous cell differentiation. Keratin 14 (K14) is expressed in mitotically active basal layer cells, along with its partner keratin 5 (K5), and their expression is down-regulated as cells differentiate. Apart from the cytoprotective functions of K14, very little is known about K14 regulatory functions, since the K14 knockout mice show postnatal lethality. In this study, K14 expression was inhibited using RNA interference in cell lines derived from stratified epithelia to study the K14 functions in epithelial homeostasis. The K14 knockdown clones demonstrated substantial decreases in the levels of the K14 partner K5. These cells showed reduction in cell proliferation and delay in cell cycle progression, along with decreased phosphorylated Akt levels. K14 knockdown cells also exhibited enhanced levels of activated Notch1, involucrin, and K1. In addition, K14 knockdown AW13516 cells showed significant reduction in tumorigenicity. Our results suggest that K5 and K14 may have a role in maintenance of cell proliferation potential in the basal layer of stratified epithelia, modulating phosphatidylinositol 3-kinase/Akt–mediated cell proliferation and/or Notch1-dependent cell differentiation.**

Monitoring Editor
Robert David Goldman
Northwestern University

Received: Aug 17, 2010
Revised: Aug 22, 2011
Accepted: Sep 1, 2011

INTRODUCTION

Keratins (Ks) are the largest subgroup of intermediate filament (IF) proteins preferentially expressed in epithelial tissues (Moll *et al.*, 1982; Coulombe and Omary, 2002). They are subdivided into type I acidic (K9–K28) and type II basic (K1–K8 and K71–K74) keratins (Moll *et al.*, 1982; Schweizer *et al.*, 2006) on the basis of biochemical properties, such as molecular weight and isoelectric point (Hesse *et al.*, 2004). They are obligatory heteropolymers and are assembled in 1:1 molar ratio, consisting of one type I and one type II keratin (Moll *et al.*, 1982; Coulombe and Omary, 2002; Herrmann and Aebi, 2004). Epithelial tissues express different pairs of keratins depending upon the cell type, that is, all stratified squamous epithelia express K5/K14 (Nelson and Sun, 1983), while K8/K18 are seen in all simple epithelia (Omary *et al.*, 2009).

Keratins have a basic molecular structure common to all cytoplasmic IF proteins. They have a highly conserved central coil-coil α-helical "rod" domain flanked by a non–α-helical, N-terminal "head" and C-terminal "tail" domains of various lengths (Fuchs and Weber, 1994; Herrmann and Aebi, 2004). The central rod domain plays a critical role in filament assembly. The heptad-repeat structure within the central domain of keratin monomers facilitates filament formation (Albers, 1996). The point mutations in human keratin genes (in rod domain) are associated with different epithelial disorders in multiple tissue types. These inherited human diseases exhibit cytolysis of epithelial cells, resulting in blistering of the corresponding epithelial sheets (Fuchs and Cleveland, 1998; Moll *et al.*, 2008). These observations, along with several studies conducted on

This article was published online ahead of print in MBoC in Press (http://www.molbiolcell.org/cgi/doi/10.1091/mbc.E10-08-0703) on September 7, 2011.

Address correspondence to: Milind M. Vaidya (mvaidya@actrec.gov.in).

Abbreviations used: EBS, epidermolysis bullosa simplex; EGFP, enhanced green fluorescent protein; ERK, extracellular signal-regulated protein kinase; FBS, fetal bovine serum; GFP, green fluorescent protein; IF, intermediate filament; IMDM, Iscove's Modified Dulbecco's Medium; K, keratin; MTT, 3-[4,5-dimethylthiazol-2-yl]-2,5-diphenyltetrazolium bromide; NICD, notch intracellular domain; OD, optical density; PARP-1, poly(ADP-ribose) polymerase-1; PCNA, proliferating cell nuclear antigen; PI3K, phosphatidylinositol 3-kinase; PKB, protein kinase B; RT-PCR, reverse transcriptase PCR; SCC, squamous cell carcinoma; shRNA, short hairpin RNA; TA, transient amplifying.

keratin knockout mice and mice carrying dominant keratin mutations, suggest that keratin filaments provide mechanical support to tissue architecture and are critical for the maintenance of cell viability (Fuchs and Cleveland, 1998; Coulombe *et al.*, 2004; Gu and Coulombe, 2007). In addition to their cytoprotective functions, they also perform some important regulatory functions by modulating certain signaling pathways (Paramio and Jorcano, 2002; Magin *et al.*, 2007). They form complex signaling platforms and interact with various proteins, such as kinases, adaptors, and receptors (Pallari and Eriksson, 2006), and thus regulate/modulate different signaling pathways associated with various cellular processes, such as protein synthesis, cell growth, and cell differentiation (Ku *et al.*, 2002; Oshima, 2002; Koch and Roop, 2004; Kim *et al.*, 2006).

In stratified epithelia, keratins exhibit a complex expression pattern tightly regulated by the differentiation program of the tissue. The keratins in the basal proliferating layer of these epithelia are K5/K14 (Moll *et al.*, 1982). As these cells move upward and differentiate, K5/K14 levels are gradually reduced and expression of a new pair of keratins is induced, depending upon the tissue type (Fuchs and Green, 1980). Differentiating cells express K1/K10 in skin; K4/13 in internal stratified epithelia, such as esophagus; and K3/K12 in corneal cells (Albers, 1996).

Keratin 14 (K14) is a prototypic marker of dividing basal keratinocytes and helps in the maintenance of epidermal cell shape; it also provides resistance to mechanical stress. Interestingly, the K5/K14 pair is expressed in the basal layer of the epidermis, which contains epidermal stem cells and transient amplifying (TA) cells, while the K1/K10 pair is synthesized only in postmitotic keratinocytes (Coulombe *et al.*, 1989; Byrne *et al.*, 1994). K14 mutations have been associated with a hereditary skin blistering disease called epidermolysis bullosa simplex (EBS; Lane, 1994; Omary *et al.*, 2004) and mice harboring a K14 null mutation also exhibit a phenotype similar to EBS (Lloyd *et al.*, 1995). K14 null mice demonstrate extensive blistering and die ~2 d after birth, indicating the functional importance of K14 in maintaining mechanical integrity of the stratified epithelial cells (Chan *et al.*, 1994; Rugg *et al.*, 1994). In addition, K14 is also implicated in regulating certain apoptosis-associated signaling pathways via TRADD (tumor necrosis factor α–associated death domain) and extracellular signal-regulated protein kinase (ERK) (Yoneda *et al.*, 2004; Lugassy *et al.*, 2008; Russell *et al.*, 2010). Transgenic and in vitro studies indicate that loss of K14 cannot be completely compensated for by the ectopic expression of other keratins (Hutton *et al.*, 1998; Paladini and Coulombe, 1998). These observations imply that the K5/K14 pair is required for normal development and functioning of the basal cells and performs some unique regulatory functions. However, unique tissue-specific functions of this pair in relation to cell proliferation and keratinocyte differentiation are not yet fully understood.

In this study, we have investigated the role of K14 in cell proliferation, differentiation, and neoplastic progression using RNA interference. K14 expression was stably inhibited in both HaCaT and AW13516 cells. K14 knockdown cells showed depletion in its normal partner K5. K14-deficient cells demonstrated substantial reduction in cell proliferation, decrease in phospho-Akt levels, increase in activated Notch1 levels, and increase in levels of keratinocyte differentiation markers. K14 knockdown also led to reduction in tumorigenic potential in AW13516 cells.

RESULTS

Generation of stable K14 knockdown cells

To generate efficient shRNA constructs for knockdown of K14, four different sequences were used to generate pTU6 PURO-based short hairpin RNA (shRNA) constructs. The constructs were validated by testing their efficiency to inhibit the expression of an exogenously expressed green fluorescent protein (GFP)-tagged K14 construct. shRNAK14.2 and shRNAK14.4 showed significant knockdown of exogenous GFP-tagged K14 expression (Supplemental Figure S1). The most effective shRNA construct (shRNAK14.4) or the empty vector control was transfected into the HaCaT and AW13516 cell lines, to obtain stable K14 knockdown and vector control clones. K14 expression (both mRNA and protein) in shRNAK14.4-transfected stable clones (shRK14-D1, -D2, and -D6 derived from HaCaT and shRK14-K7, -K9, and -K16 derived from AW13516) was determined by RT-PCR and Western blot analysis respectively. K14 expression in K14.4-shRNA transfected HaCaT stable clones (shRK14-D1, -D2, and -D6) was significantly reduced compared with the vector control (pTU6-Hac) generated upon transfection of pTU6-PURO alone (Figure 1, A and B). A substantial reduction in K14 level was also observed in shRNAK14.4-transfected AW13516 stable clones (shRK14-K7, -K9 and -K16), as compared with the vector control clone (pTU6-AW1; Figure 1, A and B). Moreover, K14 filaments were absent in K14 knockdown clones, while vector control clones showed K5/K14 filaments, as determined by confocal microscopy (Figure 1C). These clones demonstrated significant reduction in protein level (Figure 1A) and ~60% decrease in filament formation of K14's normal partner K5 (Figure 1C). K5 was still able to form some filaments, possibly because of its pairing with some other type I keratin in these cells. No significant difference in protein expression (Figure S2, A and C) and filament formation of K8 or K18 was observed in these clones (Figure S2, B and D). This observation ensures the specificity of our K14 shRNA, especially since the keratins share a great deal of homology at the sequence level.

K14 knockdown leads to reduction in cell proliferation

To determine the effects of K14 downregulation on cell proliferation, 3-[4,5-dimethylthiazol-2-yl]-2,5-diphenyltetrazolium bromide (MTT) assays were performed on the K14 knockdown (shRK14-D1 and -D2; shRK14-K7 and -K9 derived from HaCaT and AW13516, respectively) and the respective vector control clones (pTU6-HaC and pTU6-AW1). K14 knockdown in both cell lines resulted in significant reduction in cell proliferation (Figure 2, A and B). In addition, colony-forming ability of K14 knockdown and vector control clones was assessed. K14 knockdown clones demonstrated considerable reduction in colony-forming efficiency compared with their vector control clones. Moreover, the average size of colonies formed by K14 knockdown cells was smaller than for colonies formed by vector control cells (Figure 2, C and D), which correlates with the slower proliferation rate. Our results therefore suggest that K14 knockdown leads to substantial reduction in cell proliferation.

K14 knockdown cells show delayed cell cycle progression

The K14-knockdown clones (shRK14-D1 and -D2) showed decreased cell proliferation in comparison with vector control cells, as determined by MTT assay (Figure 2, A and B). To understand whether the decrease in cell proliferation was due to delay in cell cycle, we analyzed cell cycle progression through different phases at different time points by flow cytometry (Figure S3) and Western blotting. The vector control and K14 knockdown clones showed approximately the same percentage of cells in G1-phase upon serum starvation (Figure S3). However, the percentage of cells in S-phase at 18 h for K14 knockdown clones was significantly reduced compared with vector control (Figure 3A). Using Western blot analysis, we also observed reduction in the levels of cyclin D1 (G1/S phase–specific cyclin) and proliferating cell nuclear antigen (PCNA; S phase–specific

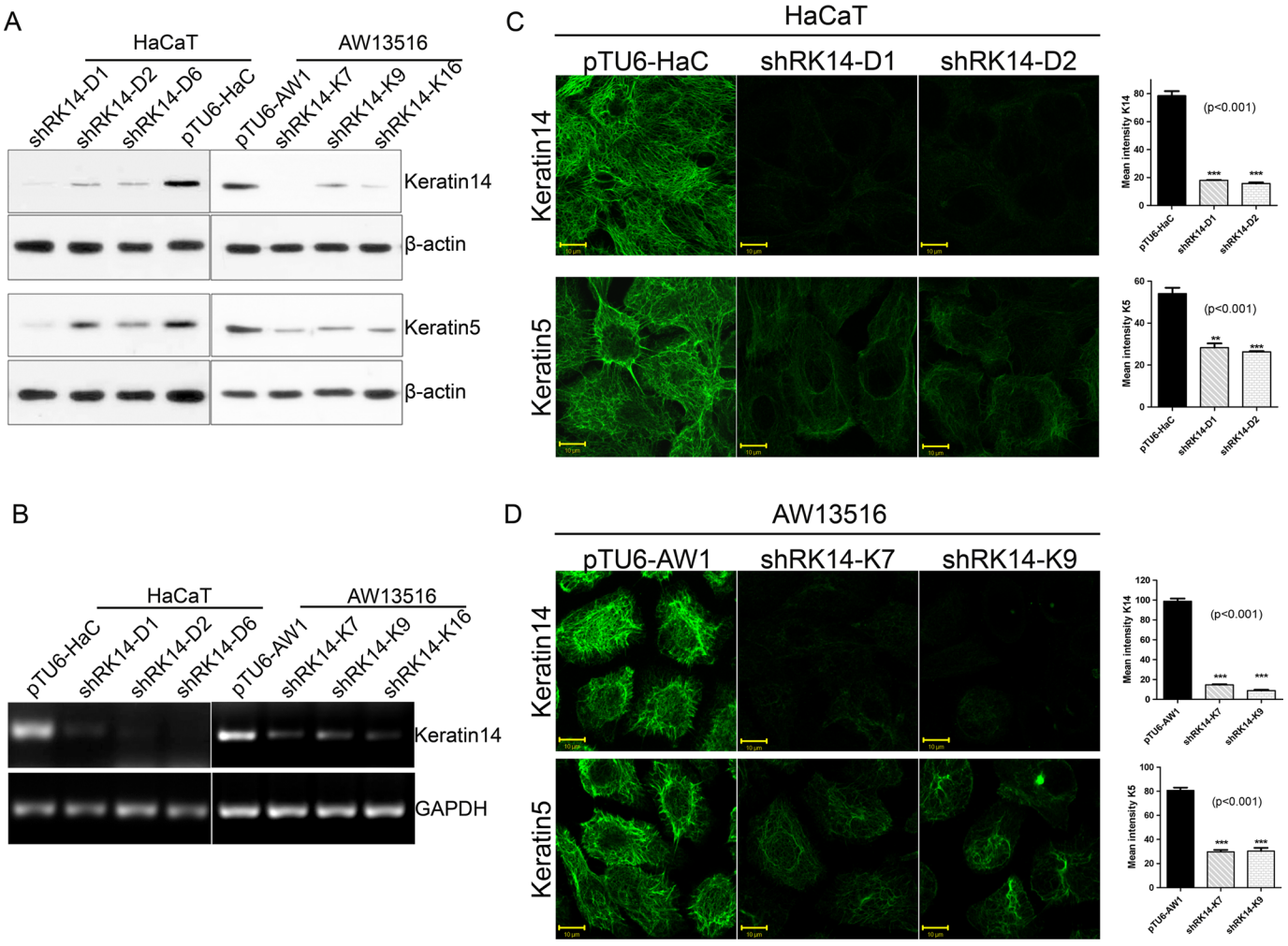

FIGURE 1: Generation of K14 knockdown clones of HaCaT and AW13516 cells. (A) Western blot analysis of stable K14 knockdown clones (shRK14-D1, -D2, and -D6 derived from HaCaT; shRK14-K7, -K9, and -K16 derived from AW13516) and vector control (pTU6-HaC and pTU6-AW1 derived from HaCaT and AW13516, respectively) cells with antibodies to K14 and K5. β-Actin was used as a loading control. (B) RT-PCR analysis of K14 in stable K14 knockdown and the respective vector control clones. GAPDH was used as internal control. (C and D) Confocal analysis of K14 and K5 levels and filament networks in the indicated clones. Scale bars: 10μm. The mean fluorescence intensity (+SD) of K5 and K14 was calculated per cell by measuring fluorescence intensity of 20 cells of each experiment (using LSM10 software; Carl Zeiss MicroImaging GmbH, Jena, Germany) and is shown in the graph on the right-hand side.***, $p < 0.001$ for K14; ***, $p < 0.001$ for K5.

marker) and increase in p21 and p27 levels (inhibitors of cyclin-dependent kinases) in K14 knockdown cells (Figure 3, B and C). In addition, our immunofluorescence analysis demonstrated decreased levels of ki67 (another S-phase marker) in K14 knockdown cells (Figure 3D). Furthermore, we observed reduction in the percentage of K14 knockdown cells entering in M phase compared with vector control cells, as analyzed by flow cytometry (Figure 3A). Western blot analysis indicated phosphorylation of histone-H3 at serine 10 (mitotic marker) was also found to be reduced in K14 knockdown cells (Figure 3B). These results suggest that K14 knockdown leads to delayed S-phase progression and late entry in M phase.

Reduced activation of Akt in K14 knockdown cells

The phosphatidylinositol 3-kinase (PI3K) pathway is known to regulate cell proliferation in epithelial cells and phosphorylation of Akt is an important downstream event of PI3K activation (Vivanco and Sawyers, 2002). Recent reports clearly suggest that keratins modulate the Akt pathway during different cellular processes (Lloyd *et al.*, 1995; Kim *et al.*, 2006; Kippenberger *et al.*, 2010; Ku *et al.*, 2011). To understand whether K14 modulates cell proliferation in these cells via the PI3K/Akt pathway, activation of Akt, that is, the level of phosphorylation of Akt, was studied using Western blot analysis. K14 knockdown cells showed significantly decreased levels of phosphorylation at serine 473 residue of Akt compared with the vector control cells, whereas total Akt expression levels remained unchanged in these cells (Figure 3E). The reduced phosphorylation of Akt upon K14 knockdown correlated well with the reduced cell proliferation rate and delay in cell cycle progression. Thus our results suggest that K14 modulates cell proliferation in stratified epithelia, possibly through the PI3K/Akt pathway.

K14 knockdown results in induction of keratinocyte differentiation

K5 and K14 are expressed in the mitotically active basal layer of stratified epithelia. When these cells move upward and differentiate, K5/K14 expression is decreased and K1/K10 expression is induced

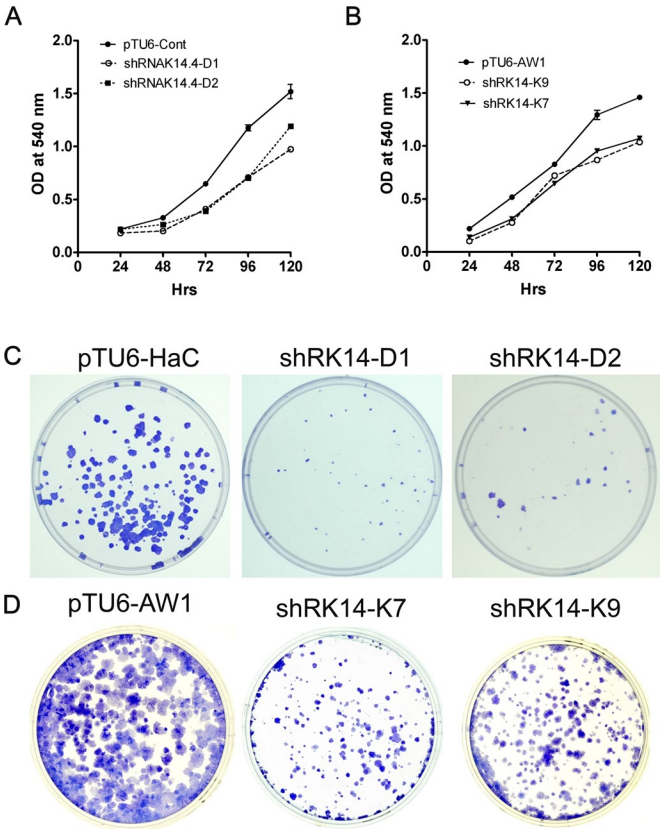

FIGURE 2: Effect of K14 knockdown on cell growth. (A and B) Cell proliferation curves of K14 knockdown and vector control cells using MTT assay. Cell proliferation was plotted against time. Results are mean ± SD of three independent experiments performed in triplicate. Note decreased cell proliferation in K14 knockdown clones. (C and D) Colony-forming assay in K14 knockdown cells. Representative images of colonies stained with crystal violet formed by the indicated clones after 14 d.

in the keratinizing layer of stratified epithelia (e.g., epidermis). This is accompanied by an inhibition of cell cycle progression and proliferation. To understand whether K14 loss leads to the phenotypic changes indicative of cell differentiation, the levels of keratinocyte differentiation markers such as involucrin and K1 were determined in K14 knockdown cells (HaCaT and AW13516) using Western blot analysis, real-time PCR and confocal microscopy. The protein levels of involucrin were significantly upregulated in K14 knockdown cells compared with vector control cells (Figure 4, A and B). Total mRNA levels of involucrin and K1 increased considerably in K14-knocdown cells (shRK14-D1 and -D2) as determined by real-time PCR (Figure 4C, D). Confocal microscopy analysis also demonstrated an increased number of involucrin- and K1-expressing cells in K14 knockdown (shRK14-D1 and -D2) compared with vector control (pTU6-Hac) clone (Figure 4E). These results indicate that depletion of K14 led to up-regulation of differentiation markers, such as involucrin and K1, in these cell lines.

K14 depletion leads to increased activation of Notch1

To investigate the possible mechanism of K14-mediated modulation of differentiation program and its associated molecules, such as involucrin and K1, we studied the Notch1 signaling pathway. As Notch1 is a key regulator of squamous cell differentiation, activated Notch1, that is, notch intracellular domain (NICD), levels were determined in K14 knockdown cells by Western blot analysis. An increase in the levels of NICD was observed in K14 knockdown clones (Figure 5, A and B). Cell surface levels of Notch1 in the K14 knockdown clones were elevated, as analyzed by confocal microscopy (Figure 5C). Furthermore, K14 knockdown cells showed increased nuclear levels of Notch1 compared with vector control cells as visualized using confocal microscopy (Figure 5D). Elevated nuclear levels of Notch1 correlated with increased NICD levels. No significant difference in mRNA levels of Notch1 and Notch2 were observed by real-time PCR in the K14 knockdown cells when compared with the vector control cells (Figure S3A). These results suggest that K14 knockdown leads to increase in NICD levels, possibly modulating the levels of differentiation markers, such as involucrin and K1. Activation of Notch1 signaling was also correlated with reduced cell proliferation.

Effect of K14 knockdown cell–extracellular matrix and cell–cell adhesion

Since cell differentiation and Notch 1 activation have been shown to be associated with cell adhesion (Watt *et al.*, 2008), we analyzed cell–extracellular matrix (ECM) and cell–cell adhesion in K14 knockdown and vector control cells (methods described in Supplemental Material). K14 knockdown cells did not show significant increase in cell adhesion to ECM substrates such as matrigel, collagen, and fibronectin in comparison with vector control cells (Figure S4C). Further, cell–cell adhesion was analyzed by hanging drop assay. The K14 knockdown cells formed smaller aggregates compared with vector control cells (Table S3).

Reduction in tumorigenicity of the K14 knockdown AW13516 cells

To determine whether reduced cell proliferation and enhanced activated-Notch1 levels resulting from K14 knockdown have any effect on tumorigenic potential of cells, in vivo tumorigenicity assays were performed. The tumorigenic potential of K14 knockdown cells was determined by tumor formation upon subcutaneous injection in nude mice. The volume and frequency of tumor formation were significantly decreased in mice injected with K14-knockdown cells (shRK14-K9 and -K16) compared with mice injected with vector control cells (pTU6-AW1; Figure 6, A and B). Immunohistochemistry was used to analyze the levels of K14 in tumors. The tumors derived from the vector control (pTU6-AW1) showed higher levels of K14 as compared with the tumors derived from the K14 knockdown clones (shRK14-K7 and -K9; Figure 6C). In summary, the results suggest that K14 depletion leads to reduction in tumorigenic potential of the cells.

Rescue of K14 knockdown phenotypes by reexpression of shRNA-resistant K14

To ensure that the phenotypic changes observed upon K14 knockdown were not due to off-target effects of the shRNA construct, a rescue experiment was performed. Resistance of mutated GFP-tagged-K14 construct (K14GFP-RR) to shRNAK14.4 was confirmed by cotransfecting it in HEK-293 cells and measuring the intensity of GFP and Western blot analysis. K14GFP-RR demonstrated resistance to shRNAK14.4 (Figure S5, A and B). To investigate the reversal in phenotypic and molecular changes, K14GFP-RR and empty vector pEGFP were transfected in a shRK14-D1 clone. Stable clones D1-pEGFP and D1-K14GFP (R11, R12) were obtained after transfection with pEGFP and K14GFP-RR, respectively. K14 expression and filament formation were analyzed by Western blotting and confocal microscopy. K14GFP-RR–transfected cells showed increased K14

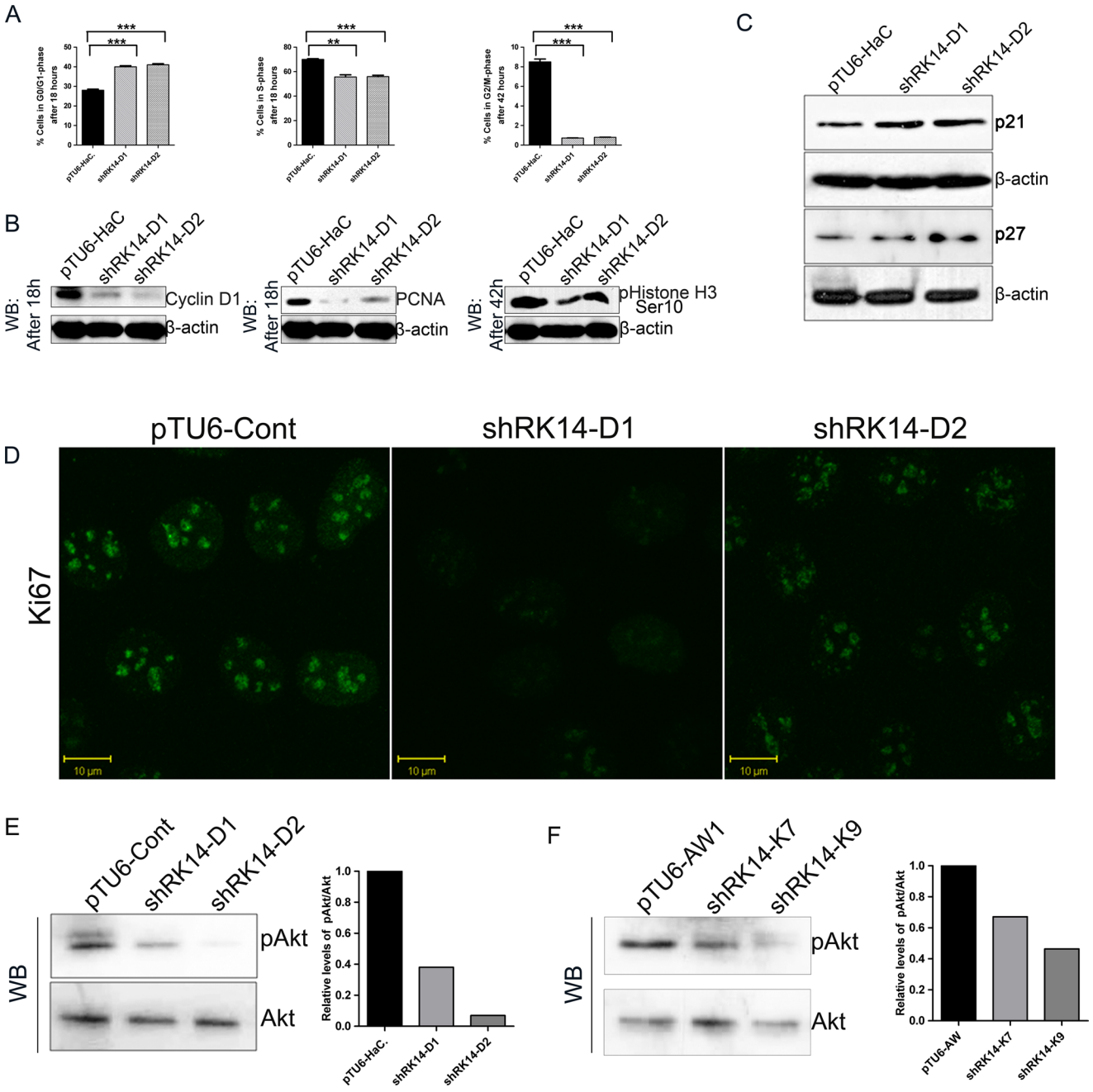

FIGURE 3: K14 knockdown resulted in delayed cell cycle progression. (A) Histograms (mean ± SD for three independent experiments) showing percentage of cells in cell cycle phases (G0/G1, S, and G2/M phase) in stable K14 knockdown and vector control clones after indicated time points, as analyzed by flow cytometry. ***, $p < 0.0001$ for G0/G1 phase; *, $p < 0.001$ for S phase; ***, $p < 0.0001$ for G2/M phase. (B and C) Western blot analysis of stable K14 knockdown clones (shRK14-D1 and shRK14-D2) and vector controls (pTU6-HaC) with antibodies to cyclin-D1, PCNA, phosphorylated histone-H3, p21, and p27. β-Actin was used as a loading control. (D) Staining of cell proliferation marker Ki67: confocal analysis of Ki67 in K14 knockdown (shRK14-D1 and shRK14-D2) and vector control (pTU6-HaC) clones. Scale bars: 10 μm. (E and F) Western blot analysis of stable K14 knockdown clones and vector control clones (shRK14-D1 and shRK14-D2 derived from HaCaT and shRK14-K7 and shRK14-K9 derived from AW13516) and the respective vector controls (pTU6-HaC and pTU6-AW1) with antibodies to phosphorylated form of Akt. Total Akt was used to validate equal loading.

and K5 levels as compared with pEGFP-transfected cells (Figure 7, A and B). GFP-tagged exogenous K14 also showed proper filament formation with its normal partner K5 in K14GFP-RR stable clones (Figure 7C). These clones demonstrated increases in both cell proliferation rate (analyzed by MTT assay; Figure 7D) and phosphorylated-Akt levels (Figure 7E). Furthermore, reduced involucrin and activated Notch1 levels were observed in K14GFP-RR–transfected cells (Figure 7E). Taken together, these results confirmed that molecular and phenotypic changes observed after K14 knockdown are due to depletion in K5 and K14 levels.

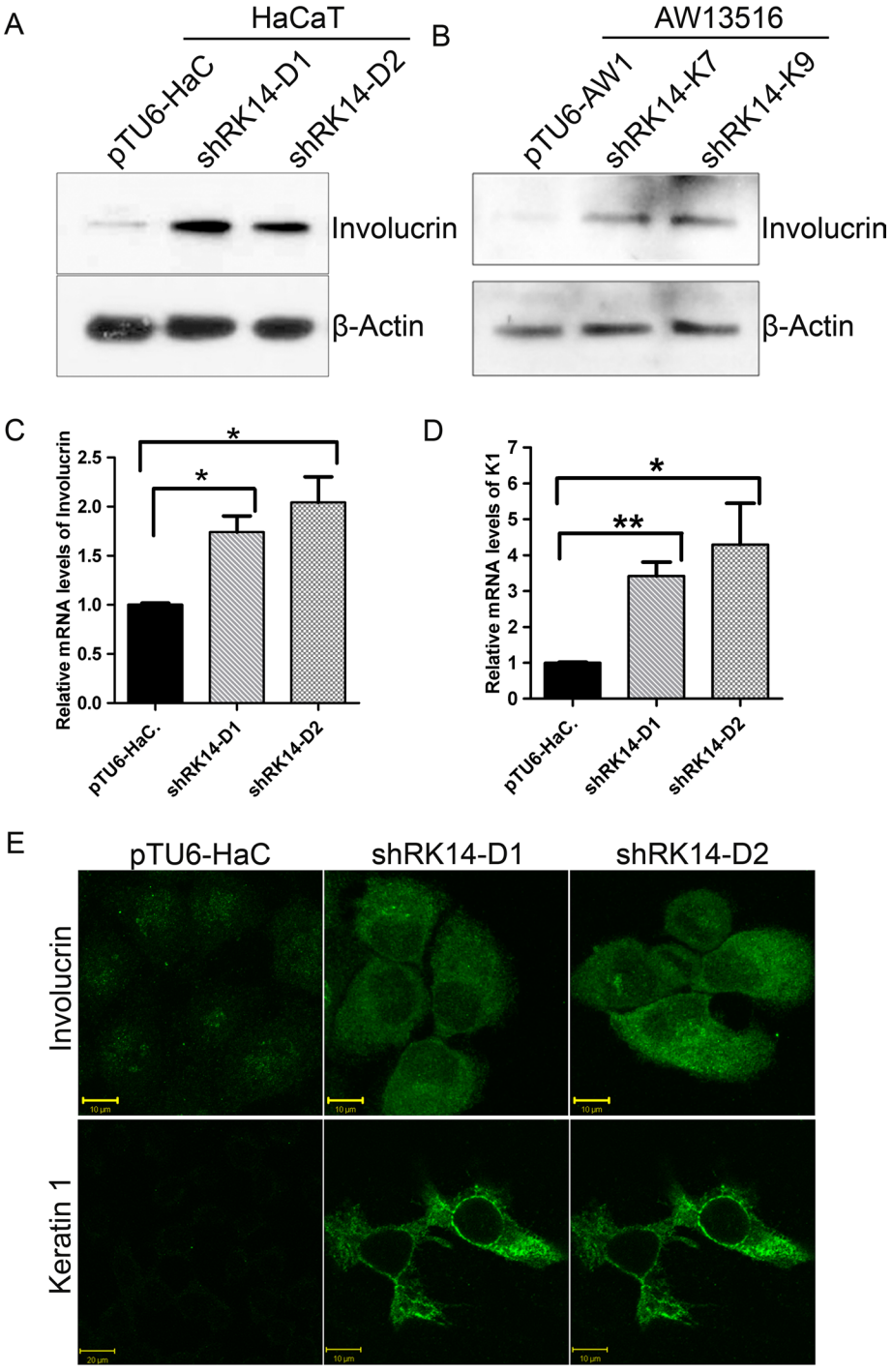

FIGURE 4: Alterations in cell differentiation–associated molecules. (A and B) Western blot analysis of stable K14 knockdown clones (shRK14-D1 and -D2; shRK14-K7 and -K9) and the respective vector control clones (pTU6-HaC and pTU6-AW1) with antibodies to involucrin. β-Actin was used as a loading control. (C) Confocal analysis of involucrin and K1 levels in the indicated clones. Scale bars: 10 μm. (D and E) mRNA levels of involucrin and K1 in indicated clones were determined by real-time PCR analysis. Levels of mRNA were normalized by GAPDH. The graph shows mean ± SD for three independent experiments done in triplicate. *, $p < 0.05$; **. $p < 0.01$.

as involucrin and K1, were also found to be increased, as was activation of Notch1 signaling in these cells. In addition, the tumorigenic potential of the K14 knockdown clones of AW13516 cells was found to be significantly reduced. Reexpression of shRNA-resistant K14 resulted in reversal of the phenotypic and molecular changes, such as increase in cell proliferation, increased phosphorylated Akt, reduction in involucrin, and a decrease in NICD levels.

DISCUSSION

The keratin 5 and 14 pair is normally expressed in the basal layer of all stratified epithelia, and its expression decreases as these cells differentiate and lose their proliferation potential. Previous in vitro and transgenic mouse model studies, where the loss of K14 cannot be completely compensated by the ectopic expression of other keratins, suggest that K14 may have some unique tissue-specific functions (Hutton *et al.*, 1998; Paladini and Coulombe, 1998) that are not yet well understood. In this study, we show decreased cell proliferation rate (Figure 2, A and B) in response to K14 knockdown. Furthermore, we also observed delayed cell cycle progression (Figure S3) and reduction in the levels of cyclin D1, PCNA, and Ki67 with concomitant increases in p21 and p27 levels (Figure 3, B and C). Consistent with these findings, K14 knockdown cells also showed delayed M-phase entry (Figure 2, A and B) and reduction in the levels of histone-H3 phosphorylation at serine 10 (Figure 3B). Previous reports have shown that K5 and K14 are specifically expressed in the mitotically active basal layer of the stratified epithelia, which contains epidermal stem cells and TA cells (Fuchs and Green, 1980). In another in vitro study, primary cultures developed from K14-null mice showed reduction in cell proliferation (Troy and Turksen, 1999). These observations suggest that K5/14 may be involved in control of cell proliferation. Our results are in agreement with these findings and provide experimental evidence for this hypothesis. To confirm that the reduction in cell proliferation seen in K14 knockdown cells was not the effect of increased apoptosis, we analyzed caspase-3 and poly(ADP-ribose) polymerase-1 (PARP-1) activity in these cells. Our results showed that there was no substantial difference in caspase-3 and PARP activities between these cells (Figure S5C). These observations suggest that K5 and K14 have some role in promoting and/or maintaining cell proliferation in basal cells.

In summary, we have shown that K14 knockdown led to drastic reduction in cell proliferation, delayed cell cycle progression, reduction in cell cycle progression markers (cyclin-D1, PCNA, Ki67, and phosphorylated-Histone-H3), and decreased phosphorylated Akt levels. Moreover, levels of keratinocyte differentiation markers, such

PI3K signaling has been shown to be a key regulator of various cellular processes, including cell growth and cell fate decisions, such as differentiation and cell survival (Vivanco and Sawyers, 2002).

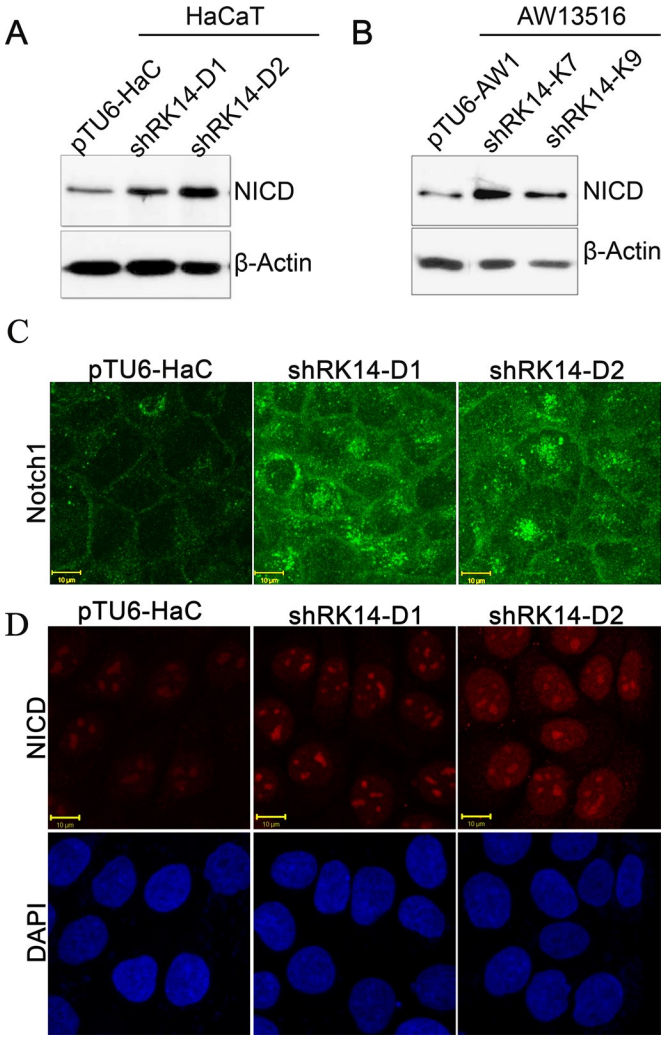

FIGURE 5: Activation of Notch1 signaling upon K14 knockdown. (A and B) Western blot analysis of stable K14 knockdown and the respective vector control clones with antibodies to NICD. β-Actin was used as a loading control. Confocal analysis of cell surface (C) and NICD (D) in the indicated clones. Scale bars: 10 μm.

The serine/threonine protein kinase Akt, also known as protein kinase B (PKB), is a downstream target of PI'3-kinase. PI'3-kinase is known to phosphorylate Ser473 residue of Akt, leading to its complete activation (Alessi *et al.*, 1997). Activated Akt then regulates several physiological and pathophysiological processes. Akt's role in maintaining normal cell proliferation, growth, and differentiation is now well established (Fayard *et al.*, 2005). Our results demonstrated that K14 depletion leads to reduction in levels of phosphorylation at Ser473 residue of Akt in these cells (Figure 3D). It has been shown in a cell line derived from an EBS patient that aggregation of K5 and K14 filaments results in activation of ERK and Akt in response to stress stimuli (Russell *et al.*, 2010). The role of some other stratified epithelial keratins like K17 in regulation of epithelial cell growth via Akt-mTOR (target of rapamycin) pathways has been depicted using the knockout mouse model. (Kim *et al.*, 2006). Studies using K10-transfected keratinocytes and K10 forced expression in the basal layer of transgenic mice suggest that K10 inhibits cell cycle entry by sequestration of Akt and protein kinase C in an Rb-dependent manner (Paramio *et al.*, 2001; Santos *et al.*, 2002). In contrast, Reichelt *et al.* (2004) have shown no increase in epidermal Akt activation in K10 knockout mice. The authors suggest that it is possible that the activation of Akt is not seen in the suprabasal layers of K10-knockout mice because activated Akt expression is restricted to basal layer of the epidermis. Recently K8 has also been shown to interact with Akt1, and regulate its phosphorylation in a glycosylation-dependent manner in simple epithelial cells (Ku *et al.*, 2011). On the basis of these findings, we hypothesized that K14 may directly interact with Akt in basal layer of stratified epithelia, thus regulating its phosphorylation. Moreover, reduction in phosphorylated Akt levels in K14-depleted cells indicates the involvement of the PI3K/Akt signaling pathway in K5/ K14-mediated modulation of cell proliferation.

During epidermal differentiation, as the cells move upward from the basal layer, K5/14 expression is down-regulated and expression of cell differentiation markers such as K1/K10 and involucrin is induced (Fuchs and Green, 1980). In this study, we found increased levels of involucrin and K1 in K14 knockdown cells (Figure 4). In a previous study, Dakir *et al.* (2008) showed that transgenic mice expressing human K14 in the lung epithelium initiated a squamous differentiation program but failed to promote squamous maturation, suggesting K14 may have a role in cell differentiation of squamous epithelia. Previously, some other keratins, such as K16 and K10, have also been shown to modulate cell proliferation/ differentiation in the transgenic mouse model (Paladini and Coulombe, 1998; Wawersik and Coulombe, 2000; Santos *et al.*, 2002; Koch and Roop, 2004). There were no alterations in terminal differentiation during fetal development in K14 and K5 knockout mice (Lloyd *et al.*, 1995; Peters *et al.*, 2001). It is possible that K14 may not be the determinant of terminal differentiation, especially during fetal development, but K5 and K14 may act as modulators of terminal differentiation in the adult stage. Our study indicates that K5 and K14 act as negative regulators of cell differentiation and thus are possible controls for the squamous differentiation program.

The process of squamous differentiation requires precision in coordinating the molecular events that lead to generation of a stratified epithelium. In recent years, increasing evidence suggests that Notch1 plays a key role in controlling epidermal proliferation and differentiation and acts as direct determinant of keratinocyte growth arrest and entry into the program of cell differentiation (Rangarajan *et al.*, 2001). Activation of Notch 1 results in release and then entry of a functionally active form of Notch1 (NICD) into the nucleus. This in turn induces expression of target genes, which leads to cell cycle arrest and initiation of cell differentiation (Bray, 2006; Watt *et al.*, 2008). Our results have documented that K14 knockdown led to an increase in levels of NICD (Figure 5) that correlated with reduced cell growth (Figures 2 and 3) and elevated levels of keratinocyte differentiation markers, like involucrin and K1 (Figure 4). We have also observed increased p21 and p27 levels, which are known to be direct targets of NICD. Activation of p21 and p27 leads to cell cycle arrest (Rangarajan *et al.*, 2001; Sriuranpong *et al.*, 2001). In a recent report, it was proposed that transgenic mice expressing K10 under K5 promoter display altered differentiation and changes in expression of the Notch family of proteins in thymic epithelial cells (Santos *et al.*, 2005). Expression of Notch pathway components is dynamic in epidermis, and most studies find that Notch expression is upregulated in the suprabasal cells. Loss of K5 and K14 expression during epidermal differentiation coincides with increased Notch expression in these cells. Thus our data indicate that the K5- and K14-mediated modulation of keratinocyte differentiation is possibly via Notch1 signaling.

Increase in tumorigenicity in response to increased cell proliferation and PI3K/Akt activation has been well documented (Vivanco

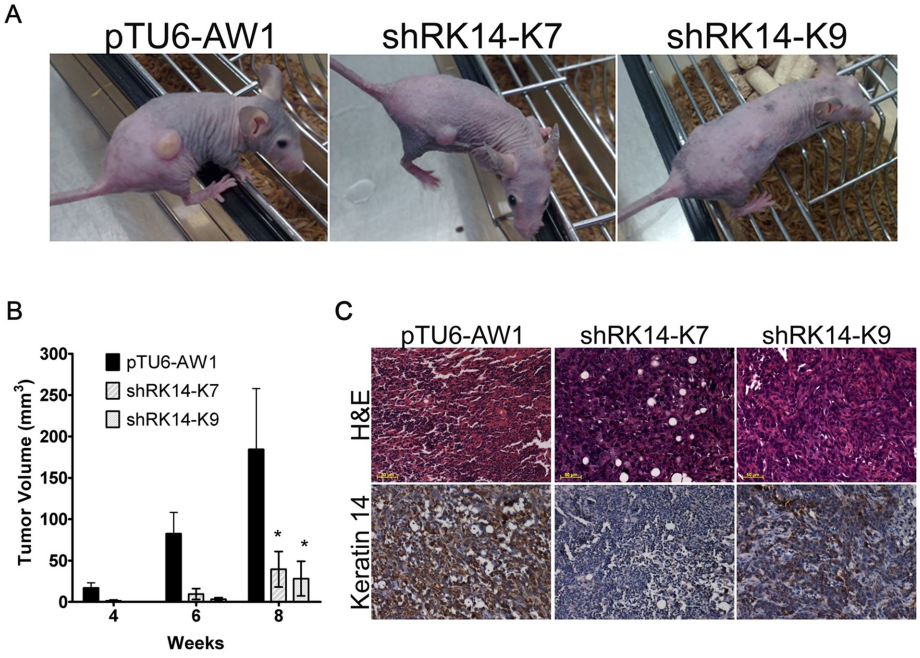

FIGURE 6: Tumorigenicity assays for K14 knockdown clones. (A) Representative images of nude mice bearing tumor of indicated clones 8 wk after the injection. (B) Tumor growth was plotted against time. Results are mean ± SD for five animals injected for each clone. Note decreased tumorigenicity in K14 knockdown clones (*, $p < 0.05$). (C) Haematoxylin and eosin along with immunohistochemical staining (with antibody against K14) of paraffin-embedded sections of tumor tissues obtained from nude mice injected with indicated clones.

and Sawyers, 2002). In addition, aberrant Notch signaling has been linked to a wide variety of tumors (Allenspach *et al.*, 2002) and its function as a tumor suppressor in the epidermis has been illustrated by transgenic studies (Proweller *et al.*, 2006; Dotto, 2008). In this study, we have demonstrated that K14 knockdown leads to reduction in tumorigenicity (Figure 6), which correlates well with decreased cell proliferation and increased Notch1 activation. Duan *et al.* (2006) have also demonstrated that constitutively overexpressed active Notch1 results in growth suppression and reduced tumorigenicity in a cell line derived from human tongue squamous cell carcinoma (SCC). These results are in agreement with our findings. It is important to note that, most SCCs show elevated K5 and K14 levels (Moll *et al.*, 1982, 1989; Moll, 1998; Chu and Weiss, 2002; Choi *et al.*, 2010). These results are suggestive of the fact that decreased tumorigenicity upon K14 depletion could be a combined effect of inhibition of the PI3K/Akt-dependent cell proliferation pathway and activation of Notch1 signaling.

Finally, reexpression of shRNA-resistant K14 in K14 knockdown cells resulted in reversal of the phenotypic and molecular changes (Figure 7), suggesting that effects observed upon K14 knockdown are specifically due to decreases in K5 and K14 levels.

In this study, we provide the first direct evidence for the involvement of K5 and K14 as modulators of cell proliferation and cell differentiation in stratified epithelia. It is apparent from our results that K5 and K14 modulate cell proliferation via PI3K/Akt pathway. In addition, K5 and K14 negatively regulate the cell differentiation program through the Notch 1 signaling pathway. It is also possible that K5 and K14 may promote neoplastic progression in oral SCC by modulating PI3K/Akt and Notch1 signaling. It will be interesting to understand the molecular basis of K5/K14-mediated regulation of cell proliferation and differentiation. Future studies using conditional knockout model will give us insights into the exact function of K5 and K14 in cell proliferation. This model will also provide a better system for studying the role of K5 and K14 in a differentiation program and lead to new information regarding stratification of these epithelia.

MATERIALS AND METHODS

Cell lines and reagents

HaCaT (derived from normal human skin) and HEK293 (ATCC) cells were cultured in DMEM (Gibco, Invitrogen, Carlsbad, CA) supplemented with 10% fetal bovine serum (FBS; Hyclone, Thermo Scientific, Lafayette, CO), and antibiotics (12.5 U/ml penicillin, 4 µg/ml streptomycin 0.05 µg/ml amphotericin B) at 37°C and 5% CO_2. The cell line AW13516 derived from the SCC of human tongue was cultured in Iscove's Modified Dulbecco's Medium (IMDM; Gibco; Tatake *et al.*, 1990) supplemented with 10% FBS (Hyclone) and antibiotics at 37°C and 5% CO_2.

Plasmids and constructs

To generate the shRNA vector constructs, four 21- to 23-nucleotide-long sequences were selected from the cDNA sequence of K14 (Supplemental Table S1). The selected sequences were analyzed by BLAST search (http://blast.ncbi.nlm.nih.gov/Blast.cgi) to ensure their specificity to their target mRNA. The oligonucleotides for K14 shRNAs (synthesized by Sigma-Aldrich, St. Louis, MO) were cloned in pTU6 PURO vector downstream of a U6 promoter digested with *Xho*I and *Age*I as described previously (Kundu *et al.*, 2008). To create the GFP-tagged K14 construct, K14 (a kind gift from Kozo Yoneda, Departments of Dermatology and Physiology, Akita University School of Medicine, Akita, Japan) was subcloned in pEGFP-N3 (Clontech, Mountain View, CA) and digested with *Xba*I and *Bam*HI.

Validation of shRNAs and selection of stable clones

To select the most effective shRNA construct, we cotransfected 1 µg of shRNA constructs with GFP-tagged K14 plasmid in HEK293 cells using the calcium phosphate precipitation method described previously (Alam *et al.*, 2011). Efficiency of knockdown was checked by green fluorescence intensity and Western blot analysis of exogenous K14-GFP 50 h posttransfection. To generate stable K14 knockdown clones, 2 µg of shRNA constructs or the empty vector were transfected into HaCaT and AW13516 cells using liposome-based FuGENE HD transfection reagent (Roche, Indianapolis, IN), and stable clones were selected in 0.5 µg/ml puromycin-containing medium (according to the manufacturer's protocol).

Site-directed mutagenesis and validation of mutant

shRNA-resistant GFP-tagged K14 construct was generated by introducing a silent mutation in the target sequence of shRNAs using the Quick change site-directed mutagenesis kit (Stratagene, Agilent, Santa Clara, CA). Oligonucleotides 5'CAGCGAGCTGGTGCAATCCGGCAAGAGCGAGATCTCG3' from Sigma) were designed according to the manufacturer's protocol. The resulting mutant construct was verified by direct DNA sequencing. To determine the resistance of the resultant mutant, we cotransfected mutated GFP-tagged K14 construct and shRNA K14.4 in HEK293 cells. Expression

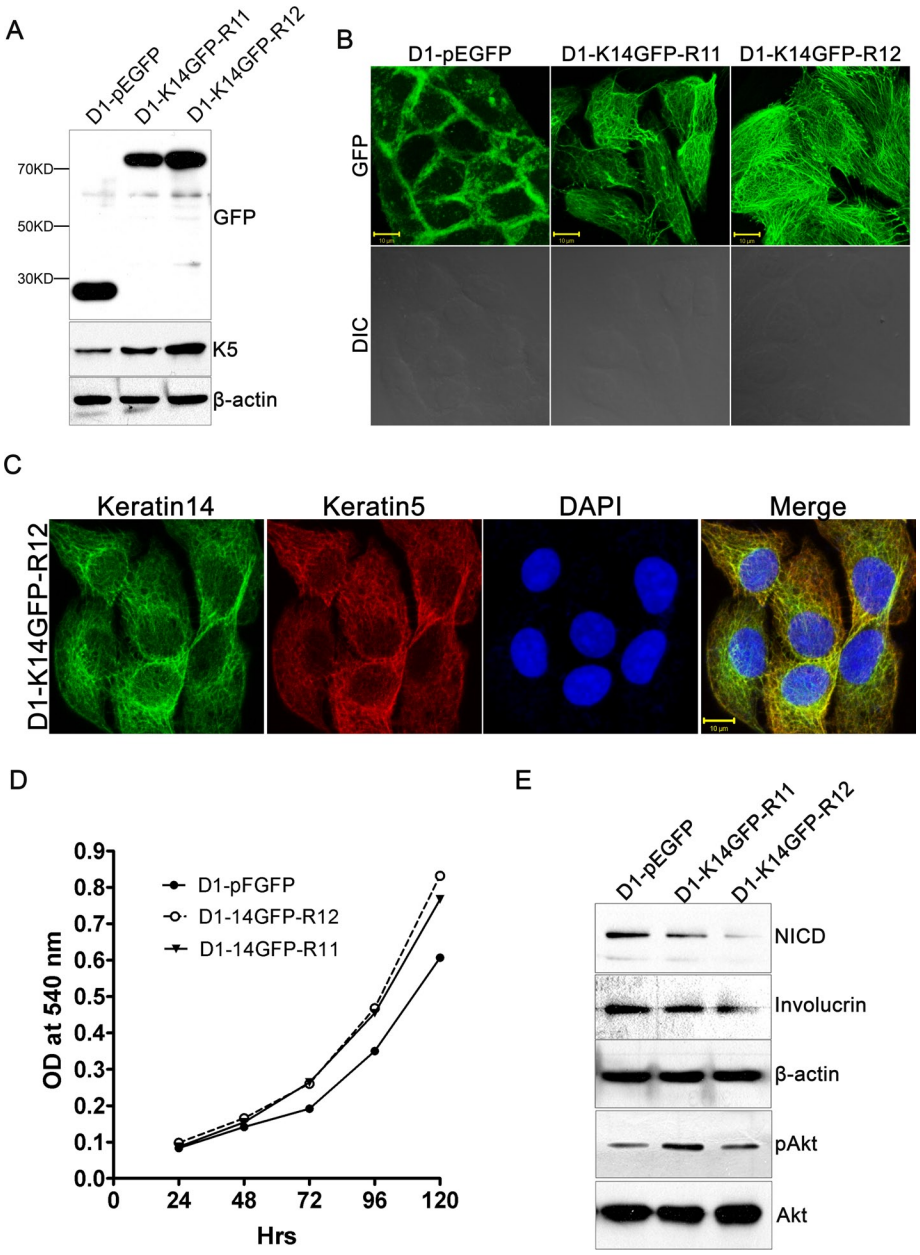

FIGURE 7: Rescue of molecular and phenotypic changes of K14 knockdown cells. (A and E) Western blot analysis of stable K14GFP-R clones (D1-K14GFP-R11 and -R12) and pEGFP clone (D1-pEGFP) derived from K14 knockdown clone shRK14-D1 cells with antibodies to GFP, K5, involucrin, Notch1, and phosphorylated form of Akt. Total Akt was used as loading control for the phosphorylated form of Akt while β-actin was used as loading control for the rest of the antibodies. (B) Confocal analysis of EGFP-tagged K14 and EGFP of the indicated clones. (C) Analysis of filament formation of EGFP-tagged K14 with K5 in the indicated clone using confocal microscopy. (D) Cell proliferation curve of D1-K14GFP-R11, -R12 and D1-pEGFP determined by MTT assay. The graph shows mean ± SD of three independent experiments performed in triplicate.

of exogenous mutated GFP-tagged K14 was examined by fluorescence and Western blot analysis 50 h posttransfection.

Western blot analysis

Whole-cell lysates were prepared in SDS lysis buffer (2% SDS, 50 mM Tris-HCl, pH 6.8, 0.1% BME, and 10% glycerol) with protease inhibitor cocktail (Calbiochem, San Diego, CA). An equal amount of protein (20 μg per well) was loaded and run on SDS–PAGE. The gels were transferred on polyvinylidene difluoride membrane (Amersham Hybond, GE Healthcare, Waukesha, WI) and probed first with the primary antibody and then with the secondary antibody conjugated with horseradish peroxidase (HRP; Amersham Pharmacia Biotech, Uppsala, Sweden). The signals were detected by using ECL Plus detection system (Amersham) according to the manufacturer's protocol.

Antibodies

The following antibodies were used: K14 (mouse monoclonal, clone LL002; AbD Serotec, Oxford, UK; working dilution 1:5000), K5 (mouse monoclonal, clone XM26; working dilution 1:1000; NovoCastra, Newcastle, UK), K8 (mouse monoclonal, clone M20; working dilution 1:5000; Sigma, St. Louis, MO) K18 (mouse monoclonal, clone CY-90; working dilution 1:10,000; Sigma), β-actin (mouse monoclonal, clone AC-74; working dilution 1:8000; Sigma), phosphoAkt (rabbit polyclonal; working dilution 1:1000; Abcam, Cambridge, UK), Akt (rabbit polyclonal; working dilution 1:1000; Abcam), Notch 1 (rabbit polyclonal, working dilution 1:1000; Abcam), Notch1 (sheep polyclonal; working dilution 1:1000; R&D Systems, Minneapolis, MN), Ki67 (mouse monoclonal; NovoCastra; Bond ready to use), p21 (rabbit polyclonal, clone C-19; working dilution 1: 200; Santa Cruz Biotechnology, Santa Cruz, CA), p27 (rabbit polyclonal, clone C-19; working dilution 1:100; Santa Cruz Biotechnology), secondary antibody HRP-conjugated anti-mouse, anti-rabbit (working dilution 1:8000; GE Healthcare UK), anti-sheep (working dilution 1:2000; Sigma).

Immunofluorescence and laser confocal microscopy

To detect the localization of proteins and filament organization of keratins in cells, immunofluorescence assay was performed as described previously (Raul *et al.*, 2004). Working dilutions for different antibodies were as follows K5, K14, K8, and K18: 1:200; Notch1, p63, involucrin, and K1: 1:100; and Ki67 was ready to use (antibody details described in *Antibodies*). The secondary antibodies, Alexa Fluor 488–conjugated anti–mouse immunoglobulin G (IgG) and Alexa Fluor 568–conjugated anti–rabbit IgG (Molecular Probes, Eugene, OR) and fluoroscein isothiocyanate (FITC)-conjugated anti–sheep IgG (BD Biosciences), were used at a dilution of 1:200. Confocal images were obtained using a LSM 510 Meta Carl Zeiss confocal system (Carl Zeiss MicroImaging GmbH, Jena, Germany).

RNA isolation and reverse transcriptase PCR

RNA was isolated by TRI reagent (Sigma), and RT-PCR was conducted using the RevertAid First Strand cDNA Synthesis Kit

(Fermentas, Thermo Scientific, Waltham, MA) according to the manufacturer's protocol. The primers used to amplify K14 and GAPDH (as internal control) and product size are shown in Supplemental Table S2. RT-PCR conditions were as follows: denaturation at 94°C for 30 s; annealing at 56°C and 58°C for K14 and GAPDH, respectively, for 30 s; and extension at 72°C for 60 s. RT-PCR products were run on agarose gel electrophoresis to compare RNA levels.

Real-time quantitative PCR

cDNA was prepared as described in the preceding section and used as templates for PCR. SYBR Green Master Mix (Applied Biosystems, Bedford, MA) was used with 200 nM of forward and reverse primers (Supplemental Table S3). Real-time quantitative PCR was performed with the ABI PRISM7700 Sequence Detection System. A standard curve was generated for each primer pair, and genes of interest were assigned a relative expression value interpolated from this standard curve using the cycle threshold, as per standard protocol. All expression values were normalized against GAPDH and β-actin. All amplifications were done three times in triplicate.

Cell proliferation assay (MTT assay)

Cells were seeded (n = 1500 cells per well), in triplicate in a 96-well microtiter plate in 100 µl complete medium. Proliferation was studied every 24 h up to a period of 5 d using MTT assay. At the desired time points, 100 µl of the medium was replenished from the designated wells, and 20 µl MTT solution was added to each well. The plate was incubated at 37°C in a CO2 incubator for 4 h, then 100 µl of acidified SDS (10% SDS in 0.01 N HCl) was added to each well, and the plate was incubated overnight at 37°C. The next day, the optical density (OD) was measured on an enzyme-linked immunosorbent assay plate reader at 540 nm against a reference wavelength of 690 nm. A growth curve was prepared from three independent experiments by plotting OD at 540 nm (on *y*-axis) against time (on *x*-axis).

Colony-forming assay

Cells (n = 400) were plated in 60-mm tissue culture plates in triplicate. Cells were grown in complete DMEM/IMDM medium for 14 d, with medium changes every 2–3 d. Cells were fixed with 4% paraformaldehyde for 1 h, which was followed by staining with 0.5% crystal violet (Himedia, in 70% ethanol) for 1 h at room temperature. Stained plates were then washed with 1X PBS, and images were captured using a high-resolution Nikon D70 camera (Nikon, Tokyo, Japan).

Cell cycle analysis

For cell cycle analysis, cells were plated in 60-mm dishes at 20% confluency. The next day, the cells were serum-starved for 72 h to synchronize the cells in G1 phase. The cells were then washed twice with PBS and fed with fresh complete medium with 10% fetal bovine serum (FBS). One set of cells was kept unsynchronized (with 10% FBS) as control. Cells were harvested at the indicated time points for the next 42 h and fixed with propidium iodide as described earlier (Hosing *et al.*, 2008). Cell cycle profile was determined by flow cytometry. Ten thousand events were acquired per plate. The data were analyzed using ModFit software (Verity, Topsham, ME).

Tumor formation in nude mice

To test the tumorigenicity of the cells, NMRI nude mice (6–8 wk old) were used. AW135167 clones (both K14-knockdown and vector control cells) were suspended in plain IMDM without serum, 3 × 106 cells were injected subcutaneously in the dorsal flank of 6- to 8-wk-old NMRI nude mice. Six mice were injected for each clone and were observed for 2 mo for tumor formation. The ellipsoid volume formula ½ × l × w × h was used to calculate the tumor volume (Tomayko and Reynolds, 1989). All protocols for animal studies were reviewed and approved by the Institutional Animal Ethics committee constituted under the guidelines of the Committee for the Purpose of Control and Supervision of Experiments on Animals, Government of India.

Histology and immunohistochemistry

The mice were killed 8 wk after subcutaneous injection, and the tumor tissues were fixed in 10% Formalin buffer and processed for histology. Five-micron sections of Formalin-fixed and paraffin-embedded tissues were stained with hematoxylin/eosin for histology. Immunohistochemical staining was performed as described previously (Ranganathan *et al.*, 2006). Signals were detected by an avidin-biotin–based immunoperoxidase technique (Elite ABC Kit; Vector Laboratories, Burlingame, CA).

Statistical analysis

Two groups of data were statistically analyzed by *t* test using GraphPad Prism 5 software (La Jolla, CA). A p value less than 0.05 was considered statistically significant.

ACKNOWLEDGMENTS

We thank Kozo Yoneda for his generous gift of the K14 construct. This work was supported by grant from the Department of Biotechnology (DBT). H.A., S.T.K., and L.S. were supported by fellowships from the Council of Scientific and Industrial Research, University Grants Commission, and DBT, Government of India, respectively.

REFERENCES

Alam H, Kundu ST, Dalal SN, Vaidya MM (2011). Loss of keratins 8 and 18 leads to alterations in alpha6beta4-integrin-mediated signalling and decreased neoplastic progression in an oral-tumour-derived cell line. J Cell Sci 124, 2096–2115.

Albers KM (1996). Keratin biochemistry. Clin Dermatol 14, 309–320.

Alessi DR, James SR, Downes CP, Holmes AB, Gaffney PR, Reese CB, Cohen P (1997). Characterization of a 3-phosphoinositide-dependent protein kinase which phosphorylates and activates protein kinase Bα. Curr Biol 7, 261–269.

Allenspach EJ, Maillard I, Aster JC, Pear WS (2002). Notch signaling in cancer. Cancer Biol Therapy 1, 466–476.

Bray SJ (2006). Notch signalling: a simple pathway becomes complex. Nat Rev 7, 678–689.

Byrne C, Tainsky M, Fuchs E (1994). Programming gene expression in developing epidermis. Development 120, 2369–2383.

Chan Y, Anton-Lamprecht I, Yu QC, Jackel A, Zabel B, Ernst JP, Fuchs E (1994). A human keratin 14 "knockout": the absence of K14 leads to severe epidermolysis bullosa simplex and a function for an intermediate filament protein. Genes Dev 8, 2574–2587.

Choi KH, Kim GM, Kim SY (2010). The keratin-14 expression in actinic keratosis and squamous cell carcinoma: is this a prognostic factor for tumor progression? Cancer Res Treat 42, 107–114.

Chu PG, Weiss LM (2002). Keratin expression in human tissues and neoplasms. Histopathology 40, 403–439.

Coulombe PA, Kopan R, Fuchs E (1989). Expression of keratin K14 in the epidermis and hair follicle: insights into complex programs of differentiation. J Cell Biol 109, 2295–2312.

Coulombe PA, Omary MB (2002). "Hard" and "soft" principles defining the structure, function and regulation of keratin intermediate filaments. Curr Opin Cell Biol 14, 110–122.

Coulombe PA, Tong X, Mazzalupo S, Wang Z, Wong P (2004). Great promises yet to be fulfilled: defining keratin intermediate filament function in vivo. Eur J Cell Biol 83, 735–746.

Dakir EL, Feigenbaum L, Linnoila RI (2008). Constitutive expression of human keratin 14 gene in mouse lung induces premalignant lesions and squamous differentiation. Carcinogenesis 29, 2377–2384.

Dotto GP (2008). Notch tumor suppressor function. Oncogene 27, 5115–5123.

Duan L, Yao J, Wu X, Fan M (2006). Growth suppression induced by Notch1 activation involves Wnt-beta-catenin down-regulation in human tongue carcinoma cells. Biol Cell 98, 479–490.
Fayard E, Tintignac LA, Baudry A, Hemmings BA (2005). Protein kinase B/Akt at a glance. J Cell Sci 118, 5675–5678.
Fuchs E, Cleveland DW (1998). A structural scaffolding of intermediate filaments in health and disease. Science 279, 514–519.
Fuchs E, Green H (1980). Changes in keratin gene expression during terminal differentiation of the keratinocyte. Cell 19, 1033–1042.
Fuchs E, Weber K (1994). Intermediate filaments: structure, dynamics, function, and disease. Annu Rev Biochem 63, 345–382.
Gu LH, Coulombe PA (2007). Keratin function in skin epithelia: a broadening palette with surprising shades. Curr Opin Cell Biol 19, 13–23.
Herrmann H, Aebi U (2004). Intermediate filaments: molecular structure, assembly mechanism, and integration into functionally distinct intracellular scaffolds. Annu Rev Biochem 73, 749–789.
Hesse M, Zimek A, Weber K, Magin TM (2004). Comprehensive analysis of keratin gene clusters in humans and rodents. Eur J Cell Biol 83, 19–26.
Hosing AS, Kundu ST, Dalal SN (2008). 14-3-3 Gamma is required to enforce both the incomplete S phase and G2 DNA damage checkpoints. Cell Cycle 7, 3171–3179.
Hutton E, Paladini RD, Yu QC, Yen M, Coulombe PA, Fuchs E (1998). Functional differences between keratins of stratified and simple epithelia. J Cell Biol 143, 487–499.
Kim S, Wong P, Coulombe PA (2006). A keratin cytoskeletal protein regulates protein synthesis and epithelial cell growth. Nature 441, 362–365.
Kippenberger S, Hofmann M, Zoller N, Thaci D, Muller J, Kaufmann R, Bernd A (2010). Ligation of beta(4) integrins activates PKB/Akt and ERK1/2 by distinct pathways—relevance of the keratin filament. Biochim Biophys Acta 1803, 940–950.
Koch PJ, Roop DR (2004). The role of keratins in epidermal development and homeostasis—going beyond the obvious. J Invest Dermatol 123, x-xi.
Ku NO, Michie S, Resurreccion EZ, Broome RL, Omary MB (2002). Keratin binding to 14-3-3 proteins modulates keratin filaments and hepatocyte mitotic progression. Proc Natl Acad Sci USA 99, 4373–4378.
Ku NO, Toivola DM, Strnad P, Omary MB (2011). Cytoskeletal keratin glycosylation protects epithelial tissue from injury. Nat Cell Biol 12, 876–885.
Kundu ST, Gosavi P, Khapare N, Patel R, Hosing AS, Maru GB, Ingle A, Decaprio JA, Dalal SN (2008). Plakophilin3 downregulation leads to a decrease in cell adhesion and promotes metastasis. Int J Cancer 123, 2303–2314.
Lane EB (1994). Keratin diseases. Curr Opin Genet Dev 4, 412–418.
Lloyd C, Yu QC, Cheng J, Turksen K, Degenstein L, Hutton E, Fuchs E (1995). The basal keratin network of stratified squamous epithelia: defining K15 function in the absence of K14. J Cell Biol 129, 1329–1344.
Lugassy J *et al.* (2008). KRT14 haploinsufficiency results in increased susceptibility of keratinocytes to TNF-α-induced apoptosis and causes Naegeli-Franceschetti-Jadassohn syndrome. J Invest Dermatol 128, 1517–1524.
Magin TM, Vijayaraj P, Leube RE (2007). Structural and regulatory functions of keratins. Exp Cell Res 313, 2021–2032.
Moll R (1998). Cytokeratins as markers of differentiation in the diagnosis of epithelial tumors. Sub-Cell Biochem 31, 205–262.
Moll R, Dhouailly D, Sun TT (1989). Expression of keratin 5 as a distinctive feature of epithelial and biphasic mesotheliomas. An immunohistochemical study using monoclonal antibody AE14. Virchows Archiv 58, 129–145.
Moll R, Divo M, Langbein L (2008). The human keratins: biology and pathology. Histochem Cell Biol 129, 705–733.
Moll R, Franke WW, Schiller DL, Geiger B, Krepler R (1982). The catalog of human cytokeratins: patterns of expression in normal epithelia, tumors and cultured cells. Cell 31, 11–24.
Nelson WG, Sun TT (1983). The 50- and 58-kdalton keratin classes as molecular markers for stratified squamous epithelia: cell culture studies. J Cell Biol 97, 244–251.
Omary MB, Coulombe PA, McLean WH (2004). Intermediate filament proteins and their associated diseases. N Engl J Med 351, 2087–2100.
Omary MB, Ku NO, Strnad P, Hanada S (2009). Toward unraveling the complexity of simple epithelial keratins in human disease. J Clin Invest 119, 1794–1805.
Oshima RG (2002). Apoptosis and keratin intermediate filaments. Cell Death Differ 9, 486–492.
Paladini RD, Coulombe PA (1998). Directed expression of keratin 16 to the progenitor basal cells of transgenic mouse skin delays skin maturation. J Cell Biol 142, 1035–1051.
Pallari HM, Eriksson JE (2006). Intermediate filaments as signaling platforms. Sci STKE 2006, pe53.
Paramio JM, Jorcano JL (2002). Beyond structure: do intermediate filaments modulate cell signalling? Bioessays 24, 836–844.
Paramio JM, Segrelles C, Ruiz S, Jorcano JL (2001). Inhibition of protein kinase B (PKB) and PKCζ mediates keratin K10-induced cell cycle arrest. Mol Cell Biol 21, 7449–7459.
Peters B, Kirfel J, Bussow H, Vidal M, Magin TM (2001). Complete cytolysis and neonatal lethality in keratin 5 knockout mice reveal its fundamental role in skin integrity and in epidermolysis bullosa simplex. Mol Biol Cell 12, 1775–1789.
Proweller A, Tu L, Lepore JJ, Cheng L, Lu MM, Seykora J, Millar SE, Pear WS, Parmacek MS (2006). Impaired notch signaling promotes de novo squamous cell carcinoma formation. Cancer Res 66, 7438–7444.
Ranganathan K, Kavitha R, Sawant SS, Vaidya MM (2006). Cytokeratin expression in oral submucous fibrosis–an immunohistochemical study. J Oral Pathol Med 35, 25–32.
Rangarajan A *et al.* (2001). Notch signaling is a direct determinant of keratinocyte growth arrest and entry into differentiation. EMBO J 20, 3427–3436.
Raul U, Sawant S, Dange P, Kalraiya R, Ingle A, Vaidya M (2004). Implications of cytokeratin 8/18 filament formation in stratified epithelial cells: induction of transformed phenotype. Int J Cancer 111, 662–668.
Reichelt J, Furstenberger G, Magin TM (2004). Loss of keratin 10 leads to mitogen-activated protein kinase (MAPK) activation, increased keratinocyte turnover, and decreased tumor formation in mice. J Invest Dermatol 123, 973–981.
Rugg EL, McLean WH, Lane EB, Pitera R, McMillan JR, Dopping-Hepenstal PJ, Navsaria HA, Leigh IM, Eady RA (1994). A functional "knockout" of human keratin 14. Genes Dev 8, 2563–2573.
Russell D, Ross H, Lane EB (2010). ERK involvement in resistance to apoptosis in keratinocytes with mutant keratin. J Invest Dermatol 130, 671–681.
Santos M, Paramio JM, Bravo A, Ramirez A, Jorcano JL (2002). The expression of keratin k10 in the basal layer of the epidermis inhibits cell proliferation and prevents skin tumorigenesis. J Biol Chem 277, 19122–19130.
Santos M, Rio P, Ruiz S, Martinez-Palacio J, Segrelles C, Lara MF, Segovia JC, Paramio JM (2005). Altered T cell differentiation and Notch signaling induced by the ectopic expression of keratin K10 in the epithelial cells of the thymus. J Cell Biochem 95, 543–558.
Schweizer J *et al.* (2006). New consensus nomenclature for mammalian keratins. J Cell Biol 174, 169–174.
Sriuranpong V, Borges MW, Ravi RK, Arnold DR, Nelkin BD, Baylin SB, Ball DW (2001). Notch signaling induces cell cycle arrest in small cell lung cancer cells. Cancer Res 61, 3200–3205.
Tatake RJ, Rajaram N, Damle RN, Balsara B, Bhisey AN, Gangal SG (1990). Establishment and characterization of four new squamous cell carcinoma cell lines derived from oral tumors. J Cancer Res Clin Oncol 116, 179–186.
Tomayko MM, Reynolds CP (1989). Determination of subcutaneous tumor size in athymic (nude) mice. Cancer Chemother Pharmacol 24, 148–154.
Troy TC, Turksen K (1999). In vitro characteristics of early epidermal progenitors isolated from keratin 14 (K14)-deficient mice: insights into the role of keratin 17 in mouse keratinocytes. J Cell Physiol 180, 409–421.
Vivanco I, Sawyers CL (2002). The phosphatidylinositol 3-kinase AKT pathway in human cancer. Nat Rev Cancer 2, 489–501.
Watt FM, Estrach S, Ambler CA (2008). Epidermal Notch signalling: differentiation, cancer and adhesion. Curr Opin Cell Biol 20, 171–179.
Wawersik M, Coulombe PA (2000). Forced expression of keratin 16 alters the adhesion, differentiation, and migration of mouse skin keratinocytes. Mol Biol Cell 11, 3315–3327.
Yoneda K, Furukawa T, Zheng YJ, Momoi T, Izawa I, Inagaki M, Manabe M, Inagaki N (2004). An autocrine/paracrine loop linking keratin 14 aggregates to tumor necrosis factor α-mediated cytotoxicity in a keratinocyte model of epidermolysis bullosa simplex. J Biol Chem 279, 7296–7303.